JOURNAL OF VIROLOGY, Feb. 2009, p. 1350–1358 Vol. 83, No. 3
0022-538X/09/$08.00+0 doi:10.1128/JVI.02169-08

Early Events during BK Virus Entry and Disassembly▽

Mengxi Jiang,[1] Johanna R. Abend,[1] Billy Tsai,[2] and Michael J. Imperiale[1]*

Department of Microbiology and Immunology and Comprehensive Cancer Center,[1] Department of Cell and Developmental Biology,[2] University of Michigan Medical School, Ann Arbor, Michigan 48109-5620

Received 14 October 2008/Accepted 17 November 2008

BK virus (BKV) is a nonenveloped, ubiquitous human polyomavirus that establishes a persistent infection in healthy individuals. It can be reactivated, however, in immunosuppressed patients and cause severe diseases, including polyomavirus nephropathy. The entry and disassembly mechanisms of BKV are not well defined. In this report, we characterized several early events during BKV infection in primary human renal proximal tubule epithelial (RPTE) cells, which are natural host cells for BKV. Our results demonstrate that BKV infection in RPTE cells involves an acidic environment relatively early during entry, followed by transport along the microtubule network to reach the endoplasmic reticulum (ER). A distinct disulfide bond isomerization and cleavage pattern of the major capsid protein VP1 was observed, which was also influenced by alterations in pH and disruption of trafficking to the ER. A dominant negative form of Derlin-1, an ER protein required for retro-translocation of certain misfolded proteins, inhibited BKV infection. Consistent with this, we detected an interaction between Derlin-1 and VP1. Finally, we show that proteasome function is also linked to BKV infection and capsid rearrangement. These results indicate that BKV early entry and disassembly are highly regulated processes involving multiple cellular components.

BK virus (BKV) is a member of the *Polyomaviridae* family, which also includes the well-studied simian virus 40 (SV40) and human JC virus (JCV) (21). Like other members of this family, BKV has a small (40 to 45 nm in diameter), nonenveloped, icosahedral capsid that contains an ~5-kb circular double-stranded DNA genome (5). BKV infection is ubiquitous in the human population and occurs during early childhood (24). Primary infection with BKV is followed by dissemination to the kidney and urinary tract, in particular to kidney tubule epithelial cells and urinary tract epithelial cells, where the virus establishes a lifelong persistent infection (9). This infection remains asymptomatic in immunocompetent individuals, but under conditions of immunosuppression, BKV can undergo reactivation resulting in viral shedding in the urine and may eventually lead to severe diseases, such as polyomavirus nephropathy in renal transplant patients and hemorrhagic cystitis in bone marrow transplant recipients (2). The incidence of BKV-related disease has greatly increased recently due to the introduction of new and more potent immunosuppressive agents and the increase in the number of transplants performed (21). No specific antiviral drugs for BKV infection are currently available, and the most common approach to control BKV reactivation is to reduce the immunosuppression, which might leave patients at risk for graft rejection (53). In addition, the immune components that are involved in controlling BKV persistence and reactivation are not well defined. Therefore, a better understanding of the BKV life cycle is warranted to aid in the design of novel, more-efficient antiviral strategies.

Based on cryo-electron microscopy analysis of BKV-like particles (26) and the crystal structures of mouse polyomavirus (MPyV) and SV40 (51, 52), the BKV major capsid protein VP1 forms the outer shell of the capsid, with the minor capsid proteins VP2 and VP3 forming a bridge linking the VP1 shell and the viral genome. A total of 360 copies of VP1 form 72 pentamers, with the C terminus of each VP1 monomer extending into adjacent pentamers to stabilize the interpentameric interactions, which are also dependent on calcium ions (Ca^{2+}) (25). Each VP1 pentamer also interacts with an internal VP2 or VP3 protein via hydrophobic interactions (51). The BKV genome can be divided into three major regions, as follows: the early region encoding the large tumor antigen (TAg) and small tumor antigen (tAg); the late region encoding the viral capsid proteins and the nonstructural agnoprotein; and the noncoding control region, which contains promoter elements for both the early and late regions and the origin of DNA replication (5). To achieve a productive infection, the viral genome has to be delivered to the nucleus, where early genes are expressed, followed by DNA replication, late protein expression, and virion assembly. The details of the many steps leading to productive BKV infection are not well defined.

The early life cycle of BKV starts with the binding of VP1 to the cellular receptors. Emerging evidence suggests that gangliosides GD1b and GT1b, both of which contain a terminal α2-8-linked sialic acid residue, serve as cellular receptors for BKV (34). Not only does BKV bind to GD1b and GT1b, as determined by a sucrose flotation assay, but addition of these gangliosides also renders resistant cells susceptible to BKV infection (34). It has also been reported that an N-linked glycoprotein with an α2-3-linked sialic acid can function as a receptor for BKV (11). Following initial attachment to the cell surface, BKV is internalized by caveola-mediated endocytosis (14, 39). Knowledge regarding subsequent trafficking events is very limited. Studies indicate that the transport of BKV relies on an intact microtubule network but is dynein independent (13, 40). Ultrastructural analysis of tissue samples from patients with polyomavirus nephropathy suggests that vesicles carrying BKV virions appear to be fused with an

* Corresponding author. Mailing address: 1150 West Medical Center Dr., 5724 Medical Science Building II, Ann Arbor, MI 48109-5620. Phone: (734) 763-9162. Fax: (734) 615-6560. E-mail: imperial@umich.edu.

▽ Published ahead of print on 26 November 2008.

elaborate tubular network that is in close proximity to, and/or continuous with, the Golgi apparatus or rough endoplasmic reticulum (ER) (10). Consistent with this observation, labeled BKV has been found to colocalize with an ER marker in cells infected in culture (40). There are still many gaps, however, in our knowledge of the intracellular trafficking pathways utilized by BKV.

A major question that remains unanswered is when and how the BKV capsid disassembles. The very low number of intact intranuclear virions compared to the number of large perinuclear viral aggregates observed by electron microscopy (EM) supports the idea that viral uncoating occurs before nuclear entry (10), although direct evidence is still lacking. For both SV40 and MPyV, the ER compartment is suggested to be the initial disassembly site (16, 29, 35, 41, 48). The ER protein disulfide isomerase or other protein disulfide isomerase-like proteins can cause conformational changes in VP1 molecules, leading to further membrane penetration or virion disassembly (35, 48). Furthermore, proteins involved in the ER-associated protein degradation (ERAD) pathway, which normally removes misfolded proteins from the ER for proteasomal degradation, have been implicated in polyomavirus trafficking (29, 48). This raises the possibility that the ERAD machinery is hijacked by polyomaviruses to escape from the ER prior to the delivery of genomes to the nucleus.

Many early BKV trafficking studies were performed in monkey-derived Vero cells (12). More recently, an in vitro cell culture system was established that allows the study of BKV lytic infection in primary human renal proximal tubule epithelial (RPTE) cells, a major cell type that BKV infects in vivo (33). BKV is able to replicate efficiently and produce infectious viral particles in these cultures (33). Therefore, this system provides an excellent model to study BKV infection in its natural host cell type, which is important because viral trafficking mechanisms are often cell type dependent. For example, both SV40 and MPyV have been shown to enter host cells by either caveola-dependent or -independent pathways, depending on the cell type used (6, 17, 43, 46). There are also contrasting results obtained in different cell types regarding the cytoskeleton requirements for SV40 or MPyV trafficking (17, 18, 44, 46, 49). It is crucial, therefore, to unravel the life cycle of BKV in its in vivo target cells.

In this report, we characterize the early entry and disassembly processes of BKV in RPTE cells and the potential contributions of the host machinery during these events. We show that BKV trafficking is highly regulated, with strict temporal and spatial requirements, including a low-pH step and the involvement of the ER. BKV displays a distinct capsid rearrangement and VP1 cleavage pattern during the course of infection, which is also associated with multiple cellular compartments. Finally, we find that components of the ERAD pathway are involved in BKV infection. Taken together, these results suggest that BKV employs specific trafficking pathways, which rely on various cellular components, to establish a productive infection.

MATERIALS AND METHODS

Cell culture. Primary human RPTE cells (Lonza) were maintained for up to six passages in renal epithelial cell growth medium (REGM; Lonza) as previously described (1). Vero cells (ATCC CCL-81) were maintained in Dulbecco's modified Eagle's medium (DMEM; Gibco) containing 10% fetal bovine serum (HyClone), 100 U/ml penicillin, and 100 μg/ml streptomycin (Cambrex). Both RPTE and Vero cells were grown at 37°C with 5% CO_2 in a humidified incubator.

Plasmids. To generate a glutathione *S*-transferase (GST)-tagged VP1 protein, the VP1 coding sequence was amplified from BKV strain TU genomic DNA using the primers BKV-VP1-for-SmaI (5′ CACCCGGGTATGGCCCCAA CCAA 3′) and BKV-VP1-rev-XhoI (5′ GGCTCGAGTTAAAGCATTTTGGT TTGCAA 3′). The PCR product was cloned into the pGEM-T Easy vector (Promega) and then subcloned into the GST expression vector pGEX-5X-1 via SmaI and XhoI restriction sites. The construct was transformed into *Escherichia coli* BL21-CodonPlus (Stratagene) for protein expression. pcDNA 3.1-Derlin1-YFP and pcDNA3.1-Derlin2-YFP were described previously (4).

Virus propagation and purification. BKV stocks were prepared as previously described (1). The resulting crude viral stocks were titrated by a fluorescent focus assay and used to infect 12 T150 flasks of Vero cells at a multiplicity of infection (MOI) of 0.1 infectious units per cell (IU/cell). Three weeks postinfection, cells were scraped off the flasks and the lysate was adjusted to pH 7.4 with HEPES (pH 8.0). The lysate was then centrifuged at 8,000 × *g* at 4°C for 30 min in an SLA-1500 rotor (Sorvall). The resulting supernatant (S1) was saved, and the pellet was resuspended in 20 ml of buffer A (10 mM HEPES [pH 7.9], 1 mM $CaCl_2$, 1 mM $MgCl_2$, 5 mM KCl). The lysate was sonicated in a sonicating water bath (Branson 2510) for 5 min at 4°C. The pH of the lysate was adjusted to 5.4 with HEPES (pH 5.0) and treated with 1 U/ml of type V neuraminidase (Sigma) at room temperature for 1 h. The pH was adjusted back to 7.4 with HEPES (pH 8.0), and the lysate was heated to 42°C for 5 min and centrifuged at 16,000 × *g* for 5 min at 4°C. The resulting supernatant (S2) was saved and the pellet was resuspended in a total volume of 2.5 ml of buffer A with 0.1% (wt/vol) sodium deoxycholate. The lysate was incubated at room temperature for 15 min with occasional vortexing and centrifuged at 16,000 × *g* for 5 min at 4°C. The final supernatant (S3) was combined with S1 and S2 and laid over a 4-ml 20% sucrose cushion in buffer A. Virus was pelleted through the sucrose cushion by centrifuging in a Beckman SW28Ti rotor for 3 h at 25,000 rpm (80,000 × *g*) at 4°C. The pellet was resuspended in 1.5 ml buffer A, loaded onto a 10-ml 1.2- to 1.4-g/cm^3 CsCl linear gradient, and centrifuged in a Beckman SW41Ti rotor for 16 h at 35,000 rpm (150,000 × *g*) at 4°C. The mature virus band was extracted and dialyzed against buffer A. BKV purified from Vero cells behaves identically to BKV purified from RPTE cells in regards to the kinetics of infection (data not shown), and the integrity of the noncoding control region was confirmed by sequencing of PCR products.

Infections. Seventy-percent-confluent RPTE cells were infected with purified BKV diluted in REGM at the indicated MOIs and incubated for 1 h at 37°C. The viral inoculum was then replaced with fresh REGM. Vero cells were infected in a similar manner, except that the cells were maintained in DMEM containing 2% fetal bovine serum, 100 U/ml penicillin, 100 μg/ml streptomycin, and 0.5 μg/ml amphotericin B (Invitrogen) during the infection. For all the time course and VP1 rearrangement experiments, infection was synchronized by prechilling the RPTE cells for 15 min at 4°C, and purified BKV was allowed to bind to the cells for 1 h at 4°C. At the end of the 1-h incubation, the viral inoculum was removed, and the cells were washed once with cold medium. Infection was initiated by addition of fresh REGM and transferring the cells to 37°C.

Drug treatments. NH_4Cl was purchased from Fisher; brefeldin A (BFA), nocodazole, and lactacystin were purchased from Sigma. All the drugs were reconstituted according to the manufacturers' recommendations. The drugs were added at the indicated time points before or during BKV infection at the following concentrations: NH_4Cl, 6.25 mM; BFA, 1.25 μg/ml; nocodazole, 7.5 μM; lactacystin, 20 μM. NH_4Cl, nocodazole, and lactacystin were left on for the time of the experiment; BFA was left on for only 2 h due to cytotoxicity, washed out, and replaced with fresh REGM. A cell metabolism WST-1 assay (Roche) was used to ensure that the drug treatments did not cause significant cytotoxic effects (data not shown).

Preparation of protein lysates. To prepare protein lysates under alkylating conditions, RPTE cells were infected at an MOI of 5 IU/cell at 4°C. At the indicated times postinfection, the medium was aspirated, and RPTE cells were detached with phosphate-buffered saline (PBS) containing 5 mM EDTA for 15 min at 37°C. The cells were then washed once with cold PBS, resuspended in PBS with 20 mM *N*-ethylmaleimide (NEM; Sigma), and incubated on ice for 45 min. The cells were pelleted at 300 × *g* for 5 min at 4°C and lysed in a Triton lysis buffer (10 mM Tris [pH 7.6], 10 mM sodium phosphate, 130 mM NaCl, 1% Triton X-100, 20 mM NEM) supplemented with 1× protease inhibitor cocktail tablet (Roche). The lysates were cleared by centrifugation at 20,000 × *g* for 45 min at 4°C. For all other experiments, total cell proteins were harvested using E1A lysis buffer (20) supplemented with 5 μg/ml phenylmethylsulfonyl fluoride, 5 μg/ml aprotinin, 5 μg/ml leupeptin, 0.05 M sodium fluoride, and 0.2 mM

sodium orthovanadate. Protein concentrations were determined by a Bio-Rad protein assay before Western blot analyses.

GST pull-down assay. *E. coli* cells expressing GST or GST-VP1 were induced with 0.1 mM IPTG (isopropyl-β-D-thiogalactopyranoside) at 16°C overnight. The cultures were harvested, resuspended in lysis buffer B (PBS, 0.1% β-mercaptoethanol, 0.1% Triton X-100, 2 mM EDTA, 1× protease inhibitor cocktail), and sonicated twice for 5 s at the setting of 2, using a 550 Sonic Dismembrator sonicator (Fisher). The lysates were cleared by centrifugation in a microcentrifuge at maximum speed for 5 min at 4°C and then incubated with 30 μl 50% glutathione Sepharose 4B beads (GE Healthcare) in a total final volume of 500 μl PBS. The proteins were allowed to bind to the beads at 4°C for 1 h by end-over-end rotation, and the beads were pelleted at 500 × *g* for 5 min. The beads were washed three times with PBS, and the proteins were eluted in 40 μl 2× sodium dodecyl sulfate (SDS) sample buffer (100 mM Tris [pH 6.8], 4% SDS, 20% glycerol, 200 mM dithiothreitol, 0.04% bromophenol blue). The proteins were separated by SDS-polyacrylamide gel electrophoresis (PAGE), and the gels were stained with ProtoBlue Safe (National Diagnostics). The amounts of the bacterial lysates bound to the beads were adjusted such that similar levels of GST and GST-VP1 were used in the pull-down reactions. To perform pull downs, RPTE cells were lysed in lysis buffer C (150 mM CH_3COOK, 4 mM $MgCl_2$, 30 mM Tris [pH 7.6], 10 mM NEM, 1% NP-40, 1× protease inhibitor cocktail) at 4°C for 30 min and cleared by centrifugation at 16,000 × *g* for 10 min. GST- or GST-VP1-bound beads were incubated with 500 μg of RPTE cell extract by end-over-end rotation at 4°C for 2 h. Beads were then washed three times with wash buffer (150 mM CH_3COOK, 4 mM $MgCl_2$, 30 mM Tris [pH 7.6], 10 mM NEM, 0.1% NP-40, 1× protease inhibitor cocktail). Proteins were eluted with 40 μl 2× SDS sample buffer and subjected to Western blot analysis.

Western blotting. Equal amounts of proteins were separated by reducing or nonreducing SDS-PAGE and transferred to a nitrocellulose membrane overnight at 60 V using wet transfer at 4°C. The membrane was subsequently blocked for 1 h at room temperature or overnight at 4°C in 5% nonfat dried milk in PBS containing 0.1% Tween 20 (PBS-T). After blocking, the membrane was incubated with primary antibodies diluted in 5% nonfat dried milk in PBS-T for 1 h at room temperature. The following antibody concentrations were used: PAb416 (20) for TAg, 1:3,000; P5G6 for VP1, 1:10,000; Ab9484 (Abcam) for GAPDH (glyceraldehyde-3-phosphate dehydrogenase), 1:10,000. The membrane was then washed three times with PBS-T and incubated with horseradish peroxidase-conjugated sheep anti-mouse antibody (Amersham) at a 1:5,000 dilution in 5% nonfat dried milk in PBS-T at room temperature for 1 h. The membrane was washed with PBS-T three times and developed using either enhanced chemiluminescence reagents (GE Healthcare) or luminol (Millipore). In the GST pull-down experiment, the anti-Derlin-1 antibody (4) was diluted 1:2,000 in PBS-T followed by incubation with horseradish peroxidase-conjugated donkey anti-rabbit (GE Healthcare) at a 1:2,000 dilution.

Immunofluorescence microscopy. At 48 h postinfection, BKV-infected RPTE cells grown on chamber slides (Nunc) were fixed in 4% paraformaldehyde (Electron Microscopy Sciences). Following three washes with PBS, cells were permeabilized by incubation in 0.1% Triton X-100 in PBS at room temperature for 5 min. Cells were then washed twice with PBS before being blocked with 5% goat serum (Vector Laboratories, Inc.) for 1 h at room temperature. After blocking, samples were incubated with a 1:200 dilution of PAb416 in 5% goat serum for 1 h at room temperature. The cells were then washed three times in PBS and incubated with a 1:100 dilution of goat anti-mouse immunoglobulin G (IgG) (whole molecule)-fluorescein isothiocyanate (Sigma) in 5% goat serum for 1 h at room temperature. After three washes in PBS, cells were mounted with Vectashield with DAPI (4′,6-diamidino-2-phenylindole) (Vector Laboratories, Inc.) and examined by standard fluorescence microscopy using an Olympus BX41 microscope with a Plan 10×/0.25 objective. A minimum of seven random fields were counted for each sample from three independent experiments. For the fluorescent focus assay, RPTE cells plated onto chamber slides were infected with 10-fold dilutions of viral lysates for 3 days at 37°C before fixation. The titer was determined by counting nine random fields in at least duplicate wells and is expressed as infectious units per ml (IU/ml). For the Derlin-1-yellow fluorescent protein (YFP) and Derlin-2-YFP transfection/infection experiments, RPTE cells were fixed 48 h postinfection and stained for TAg as described above. YFP- and TAg-positive cells were visualized using an Olympus IX70 inverted microscope with a Plan 40×/0.65 objective. The images were analyzed with the MetaMorph Premier software (Molecular Devices).

Transfection. Transfections were performed using TransIT-LT1 reagents (Mirus). Transfection complexes were prepared according to the manufacturer's instructions with a DNA-to-transfection reagent ratio of 1:3. Cells were seeded into two-well chamber slides, and each well was transfected with 0.5 μg of DNA. Transfection complexes were removed 12 h posttransfection, and the cells were washed twice with PBS before fresh REGM was added. Cells were infected 24 h posttransfection.

RESULTS

BKV infection in RPTE cells is dependent on low-pH environment and trafficking to ER. To begin our characterization of the intracellular trafficking pathway of BKV in RPTE cells, we took a pharmacological approach by treating cells with drugs that are known to disrupt distinct cellular structures or potential virus trafficking routes. All the drugs used in this study were tested by a cell viability assay to ensure that the dose and the length of treatment did not cause significant cytotoxic effects (at least 80% of the cells were viable compared to the untreated controls) (data not shown). Among the polyomavirus family, it is known that both MPyV and JCV require a low-pH step (3, 28). In contrast, SV40 is known to enter the caveosome, a pH-neutral organelle, and its infection does not rely on an acidification step (3, 43). EM analysis of kidney biopsy samples shows that BKV is associated with caveosome-like structures (10), but in Vero cells, BKV infection is pH dependent (14). To determine the pH dependence for BKV infection in RPTE cells, NH_4Cl was used to treat the cells during the course of infection. NH_4Cl is a lysosomotropic agent that can selectively enter cellular compartments with low internal pH and elevate the pH, thereby disrupting the acidification of these structures. Immunofluorescence microscopy for the early viral protein TAg was performed 48 h postinfection to assay the effects of the drug on BKV infection. Compared to the untreated samples, there was a significant decrease in the number of TAg-positive cells when NH_4Cl was present (Fig. 1). Similar results were obtained when the cells were treated with another lysosomotropic drug, chloroquine (data not shown). The inhibitory effect of NH_4Cl was independent of MOI, as a >80% reduction in infected cells was seen at both MOIs used (Fig. 1B).

We then examined whether BKV infection requires trafficking to the ER, a pH-neutral compartment (23), as has been suggested by previous microscopy studies (10, 40). BFA is a drug that inhibits the formation of COPI vesicles, which are involved mainly in retrograde transport from the Golgi apparatus to the ER (32). Due to cytotoxic effects upon longer exposure, RPTE cells were treated with BFA for only 2 h prior to infection. Even with this short period of treatment, there was a dramatic decrease in the percentage of infected cells, as assayed by TAg immunostaining (Fig. 2). Similar to the effects of NH_4Cl, the inhibition was MOI independent (Fig. 2B). Taken together, these results suggest that an acidic environment and movement to the ER compartment are necessary for BKV infection in RPTE cells.

Time course of BKV intracellular trafficking in RPTE cells. To gain a better understanding of the kinetics of BKV trafficking, a series of time course experiments was carried out in the presence of inhibitors. Infection was synchronized by adsorbing purified virus to prechilled RPTE cells at 4°C, and entry of the virus was initiated by transferring the cells to 37°C. At various time points postadsorption, drugs were added to the cells, and total protein lysates were harvested 48 h postinfection and probed for TAg by Western blotting (Fig. 3). The low-pH requirement occurred very early during infection; by

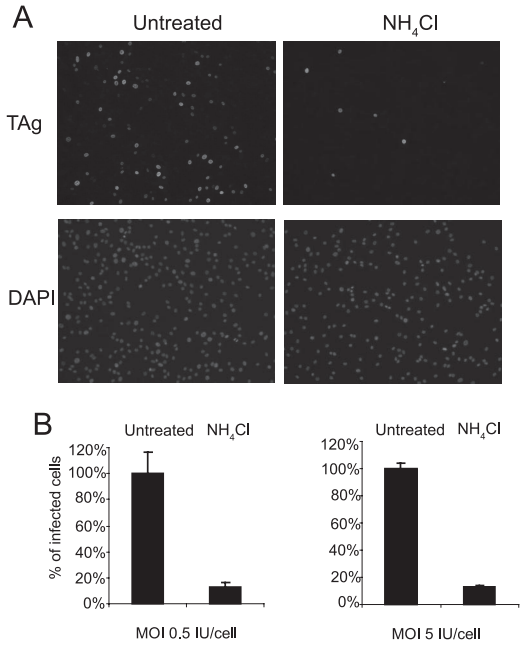

FIG. 1. BKV infection in RPTE cells requires a low-pH step. RPTE cells were either mock treated or treated with 6.25 mM NH_4Cl for 2 h at 37°C. The cells were infected with BKV at an MOI of 0.5 or 5 IU/cell for 1 h at 37°C with the drug present. The inoculum was removed after 1 h, and fresh medium with the drug was added to the cells. Cells were fixed 48 h postinfection, and infected cells were visualized by indirect immunofluorescence staining for TAg. (A) Fields of cells representing an MOI of 5 IU/cell. (B) The percentage of infected cells was normalized to that of the untreated samples. Each bar represents the mean of seven random fields from three independent experiments. The error bars are the standard deviation values.

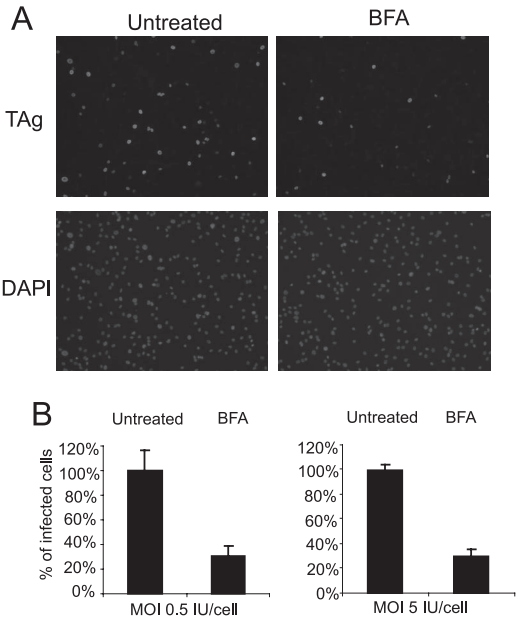

FIG. 2. BFA blocks BKV infection in RPTE cells. RPTE cells were either mock treated or treated with 1.25 μg/ml BFA for 2 h at 37°C. BFA was then washed out, and the cells were infected with purified BKV at an MOI of 0.5 or 5 IU/cell for 1 h at 37°C. The inoculum was replaced with fresh medium and the cells were stained for TAg 48 h postinfection. (A) Fields of cells representing an MOI of 5 IU/cell. (B) The percentage of infected cells was normalized to the untreated samples. Each bar represents the mean of seven random fields from three independent experiments. The error bars are the standard deviation values.

~2 h postadsorption, NH_4Cl was no longer able to inhibit TAg expression (Fig. 3A). The inhibitory effect of BFA was longer lasting, indicating that BKV reaches the ER at ~10 to 12 h postentry (Fig. 3B). Previously, it has been shown that BKV infection requires an intact microtubule network, as nocodazole, a microtubule-disrupting agent, can block TAg expression (13, 40). We therefore also included this drug in our time course experiments (Fig. 3C). The kinetics of inhibition by nocodazole was similar to that of the BFA treatment, suggesting that the virus moves along microtubules to reach the ER.

Time course of BKV capsid rearrangement in RPTE cells. Molecules of the capsid protein VP1 are cross-linked through an extensive network of interpentameric and intrapentameric disulfide bonds (27, 48), and VP1 shedding or conformational changes are believed to be the first steps of the polyomavirus disassembly process (35, 48). To monitor the BKV capsid rearrangement process, we harvested protein lysates at different time points postinfection in the presence of an alkylating agent, NEM, which prevents disulfide bond isomerization during sample preparation. The proteins were then separated by either nonreducing or reducing SDS-PAGE, followed by Western blotting for the VP1 protein using a monoclonal anti-VP1 antibody (Fig. 4). At early time points (0 to 8 h postinfection), there was no VP1 signal in the nonreducing gel, whereas full-length VP1 was detected in the reduced samples. This suggests that up to those time points, the BKV virion is still highly disulfide bonded and no VP1 molecules have been released, and therefore, VP1 cannot enter the nonreducing gel. Beginning at 8 to 12 h postinfection, a complex series of bands appeared in the nonreduced samples, and the intensity of the bands increased as the infection progressed. This likely resulted from the reduction and/or isomerization of the disulfide bonds in the capsid. At about the same time, in addition to the full-length VP1 band, two distinct faster-migrating bands were reproducibly detected in the reducing gels (denoted as VP1* and VP1**), implying that VP1 may be cleaved at specific sites during the disulfide bond rearrangement process.

Effects of NH_4Cl and BFA on BKV capsid rearrangement. We next asked whether the two inhibitory drugs, NH_4Cl and BFA, had any effects on BKV capsid rearrangement. Infection was carried out in the presence of these two drugs, and total protein lysates were prepared under alkylating conditions at 12 h postinfection, the time point at which VP1 rearrangement and cleavage were both detected (Fig. 4). The samples were subjected to nonreducing or reducing electrophoresis and probed for VP1 to assay disulfide bond rearrangement or cleavage (Fig. 5). NH_4Cl treatment completely blocked the rearrangement process, as no signals were detected in the nonreducing gel nor was either of the putative VP1 cleavage products observed in the reducing gel. Chloroquine treatment had a similar effect on VP1 rearrangement and cleavage (data not shown). When the cells were treated with BFA, however, there seemed to be an overall increase in the level of capsid rearrangement, as evidenced by a series of more intense VP1

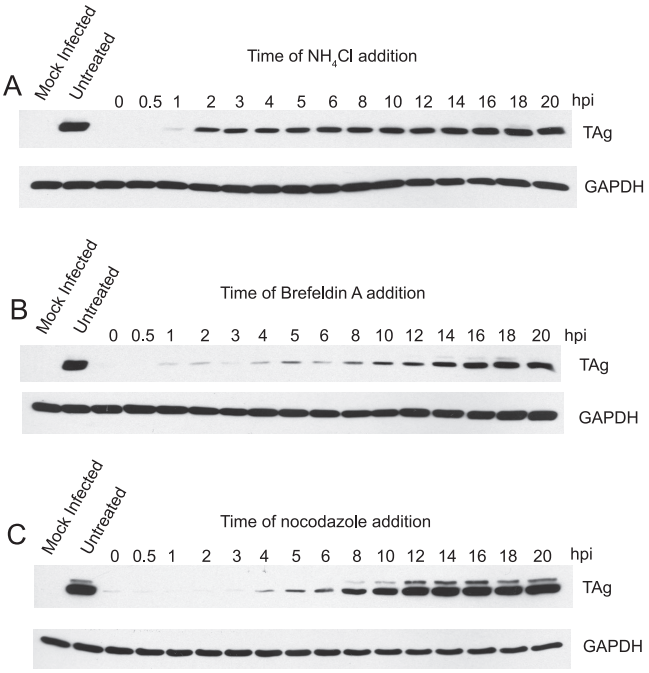

FIG. 3. Time course of BKV trafficking in RPTE cells. RPTE cells were adsorbed with purified BKV at an MOI of 0.5 IU/cell for 1 h at 4°C. Synchronized infection was initiated by shifting the cells to 37°C. At the indicated number of hours postinfection (hpi), NH_4Cl (A), BFA (B), or nocodazole (C) was added to the cells. Total cell proteins were harvested at 48 h postinfection and assayed for TAg expression by Western blotting.

bands in the nonreducing gel compared to those in the untreated sample. Correspondingly, there was a dramatic increase in the amount of VP1** in the reduced sample. There was not a dramatic change in the level of VP1*, indicating that the generation of VP1* and VP1** may occur through different routes. These results also indicate that rearrangement and cleavage of VP1 may occur prior to trafficking to the ER.

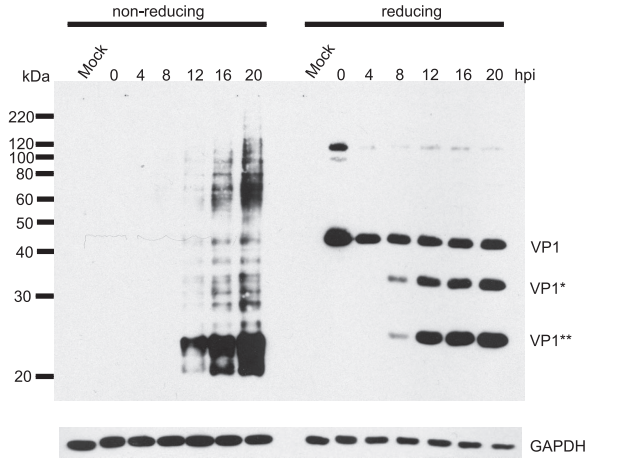

FIG. 4. Kinetics of BKV capsid rearrangement in RPTE cells. RPTE cells were infected with BKV at an MOI of 5 IU/cell, and total protein lysates were prepared at the indicated hpi under the alkylating conditions described in Materials and Methods. The proteins were separated under nonreducing or reducing conditions and probed for VP1 and GAPDH. The positions of the full-length VP1 and the two putative cleavage products, VP1* and VP1**, are shown.

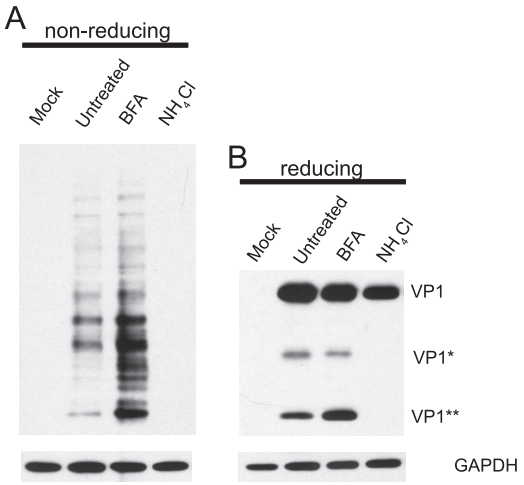

FIG. 5. Effects of BFA and NH_4Cl on BKV capsid rearrangement. RPTE cells were incubated with BKV at 4°C for 1 h at an MOI of 5 IU/cell. After the 1-h adsorption, the cells were maintained in either fresh medium or medium containing BFA or NH_4Cl. Total proteins were isolated under alkylating conditions at 12 hpi, separated under either nonreducing (A) or reducing (B) conditions, and probed for VP1 and GAPDH.

ER protein Derlin-1 is important for BKV infection. Having demonstrated BKV trafficking to the ER, we then wished to determine whether any host factors play a role in aiding BKV to escape from the ER. We first tested if Derlin proteins are involved in this process. The Derlin family proteins are ER transmembrane proteins that are important for targeting certain misfolded proteins from the ER to the cytosol for proteasome degradation, also known as the ERAD pathway (30, 31, 56, 57). Derlin-1 and Derlin-2, two members of this family, have been linked to the ER escape of SV40 and MPyV, respectively (29, 48). To investigate the possible roles of these proteins in BKV infection, RPTE cells were transfected with vectors expressing dominant negative Derlin-1 and Derlin-2 (the addition of a YFP tag converts these proteins into their dominant negative form) (4, 30). The cells were then infected with BKV and analyzed for TAg expression by immunofluorescence microscopy 48 h postinfection. The percentages of TAg-positive cells in transfected (YFP-positive) and untransfected cells were compared (Fig. 6A). A specific inhibitory effect on BKV infection was observed when the cells were transfected with Derlin-1-YFP, but not with Derlin-2-YFP. Neither Derlin-1-YFP nor Derlin-2-YFP inhibited infection of RPTE cells by adenovirus, a virus that does not traffic through the ER (37), confirming that the inhibition seen with Derlin-1-YFP was not due to general cytotoxic effects (data not shown).

To investigate a possible association between BKV and Derlin-1, a GST pull-down assay was performed to see if Derlin-1 interacts with the viral capsid protein VP1. GST or GST-VP1 was immobilized on glutathione beads and incubated with RPTE cell extracts. Complexes recovered from the beads were resolved by SDS-PAGE and probed for Derlin-1, using an anti-Derlin-1 antibody (Fig. 6B). Derlin-1 was found to be

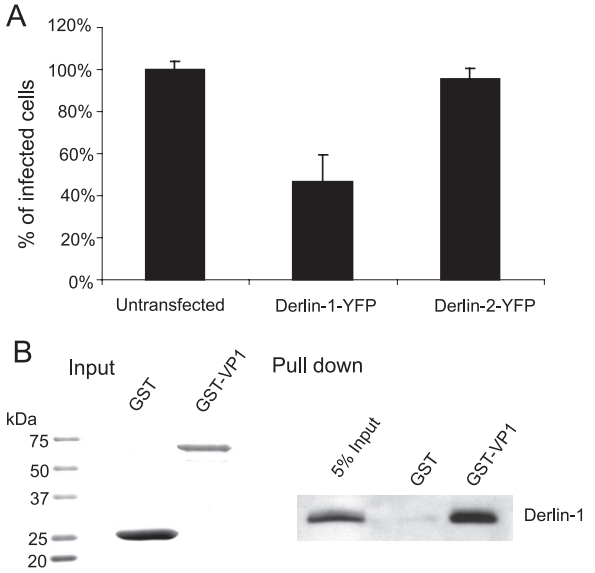

FIG. 6. Derlin-1 is required for BKV infection. (A) RPTE cells were transiently transfected with Derlin-1-YFP or Derlin-2-YFP and infected with BKV at an MOI of 0.5 IU/cell 24 h posttransfection. The cells were fixed and stained for TAg at 48 hpi. The percentage of TAg-positive cells in YFP-positive cells was normalized to that of the untransfected cells. Each bar represents the mean of the results for three independent experiments, and the error bars indicate the standard deviation values. (B) GST or GST-VP1 was bound to glutathione Sepharose beads (input shown on the left) and incubated with 500 μg uninfected RPTE cell extracts. The protein complexes recovered from the beads were probed for Derlin-1 (right). Five percent of the RPTE cell extract input is shown in the left lane.

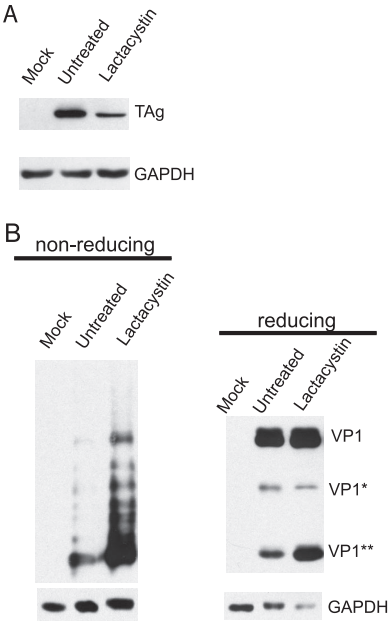

FIG. 7. The proteasome is involved in BKV infection and capsid rearrangement. (A) RPTE cells were infected with BKV at an MOI of 5 IU/cell at 4°C. After 1 h of infection, cells were maintained in fresh medium or medium containing 20 μM lactacystin. Total proteins were harvested 24 hpi and assayed for TAg expression by Western blotting. (B) RPTE cells were infected with BKV at an MOI of 5 IU/cell and treated with lactacystin. Total protein lysates were prepared under alkylating conditions at 12 hpi and analyzed as described in the legend for Fig. 5.

specifically pulled down by GST-VP1, but not by GST. These results suggest that Derlin-1 may directly participate in transporting BKV out of the ER.

Involvement of the proteasome in BKV infection and capsid rearrangement. The association between BKV and Derlin-1 led to the hypothesis that the proteasome may be involved in the infectious pathway of BKV, as Derlin-1 has been found in complexes with many of the components of the ERAD pathway (30, 31, 56, 57). Moreover, it is also possible that the proteasome participates in the disassembly process of BKV, as the ER and ERAD components have been suggested to function in the capsid rearrangement and ER escape of SV40 and MPyV (29, 48). To test this hypothesis, RPTE cells were treated with a specific proteasome inhibitor, lactacystin, which covalently binds to the β5 subunit of the 20S core particle and irreversibly inhibits proteasome activity (19). Infection was assayed by Western blotting for TAg (Fig. 7A), and capsid rearrangement was determined by blotting for VP1 under either nonreducing or reducing conditions (Fig. 7B). Lactacystin caused a significant reduction in TAg expression, suggesting that proteasome function is part of the infectious pathway. The degree of virion rearrangement, however, as judged by the amount of VP1 entering the nonreducing gel, was greatly increased in the presence of lactacystin. There was also a dramatic increase in the level of VP1** in the reducing gel, but the level of VP1* remained relatively unchanged. These results indicate that VP1 rearrangement or cleavage is not dependent on proteasome activity.

DISCUSSION

Virus entry is a complex process that involves interactions with multiple cellular compartments, transport to and from them, and different sorting pathways. A productive infection by a virus requires a proper association with its receptors, internalization into the host cell, and the delivery of its genomic content to the site of replication, all of which can be influenced by the cell types that the virus infects (36). Therefore, it is important to dissect the entry mechanism of a virus in its natural host cell type to gain the most relevant knowledge about the infectious course. In this study, we characterize several intracellular trafficking events of BKV in RPTE cells, the cell type in which the virus persists and reactivates in vivo (8). Pharmacological experiments demonstrate that BKV infection requires a low-pH step, an intact microtuble network, and trafficking to the ER. A more-detailed time course reveals the kinetics of these events, as follows: BKV travels to an acidic compartment soon after internalization, which is followed by movement along the microtubule network, presumably within a vesicular compartment, to reach the ER (Fig. 8, steps A to C).

Disassembly is another important step during polyomavirus entry, as the highly structured virion needs to be dissociated to allow entry of the genome into the nucleus. We show that the extensive disulfide bond network in the BKV capsid starts to be disintegrated at about 8 to 12 h postinfection. Interestingly, at similar times, we begin to detect two distinct, smaller fragments of VP1 that likely represent specific proteolytic cleavage products. To our knowledge, this is the first time that cleavage

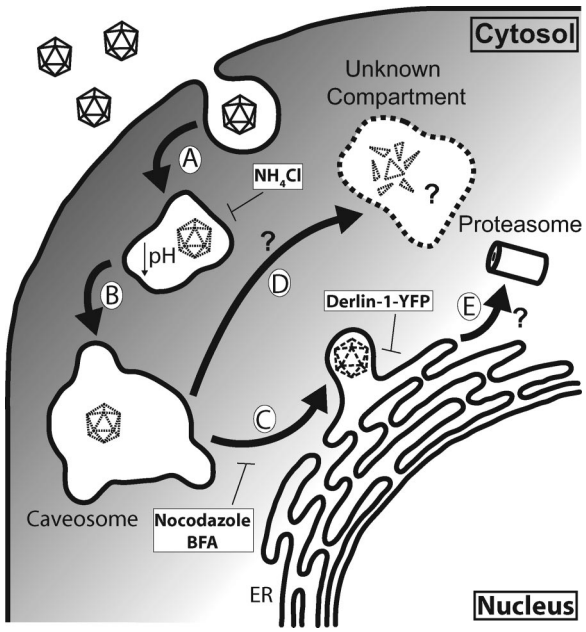

FIG. 8. Proposed model of BKV entry in RPTE cells. (A) BKV enters an acidic compartment following caveola-mediated endocytosis, where the low pH triggers conformational changes within the capsid, beginning the disassembly process. (B) BKV proceeds to the pH-neutral caveosome. (C) BKV is transported along microtubules to the ER, where it interacts with Derlin-1 to escape out of the ER. Certain conformational changes (indicated by dashed virion) may occur in the ER to aid in the escape process. (D) BKV traffics to an unknown compartment, where VP1 disulfide bond rearrangement and cleavage occur. BFA or lactacystin treatment redirects BKV toward this pathway. Whether the virus enters the proteasome through the ERAD pathway (E) remains unknown.

of the capsid protein VP1 of a polyomavirus has been observed during the course of infection. At this time, we do not know the sites of cleavage, and the epitope that the P5G6 monoclonal antibody detects is not known. Furthermore, whether the rearrangement and cleavage of VP1 molecules lead to a productive infection remains to be determined.

The endocytic events associated with BKV trafficking in RPTE cells are far from being completely understood. BKV is seen within caveosome-like structures by EM analysis (10), and the colocalization between labeled BKV and caveolin-1, a major component of the caveosome (39), supports the idea that BKV passes through the caveosome en route to the nucleus. The caveosome is a pH-neutral organelle (43); however, our results clearly show that BKV infection requires a low-pH step. In addition, colocalization between BKV and caveolin-1 peaks at ~4 h postinfection (39), which is beyond the time of the low-pH requirement. Cross talk between the caveosome and the endosomal compartments has been observed in both polyomavirus and papillomavirus infections (42, 45, 50). It is likely that an unidentified endosomal/lysosomal compartment may take part in BKV transport prior to the caveosome (Fig. 8, steps A and B). Furthermore, the role that low pH plays during BKV trafficking is still unknown. Treatment with NH_4Cl can completely block the rearrangement of the disulfide bond network within the BKV virion and VP1 cleavage. Therefore, it is likely that the low pH induces conformational changes within the capsid that lead to further virion disassembly and membrane penetration (Fig. 8, step A), as has been observed in the adenovirus endosomal escape process (55). Alternatively, the acidic pH may be required for certain cellular proteases to function, as is the case for reovirus capsid disassembly (15). It is also possible that NH_4Cl treatment traps the virus in a compartment that prevents it from further trafficking to the site of disassembly.

All the polyomaviruses that have been examined so far enter the ER compartment (10, 29, 40, 41, 43, 45); the BFA inhibition data of BKV infection are consistent with this. The ER Derlin family proteins have been implicated in the ER escape of SV40 and MPyV (29, 48). Our results show that, similar to SV40, Derlin-1 is important for BKV infection in RPTE cells. Moreover, we are able to demonstrate, for the first time, an interaction between the major capsid protein VP1 and Derlin-1. This strongly argues that Derlin-1 plays a direct role in facilitating the exit of BKV from the ER. Demonstration of an interaction between VP1 and Derlin-1 by coimmunoprecipitation during the course of infection, however, was not feasible due to the high background of VP1 adhering to the protein A/G agarose beads even with control serum (data not shown). The question that remains to be answered is whether an intact or partially disassembled virion is transported out of the ER. Derlin-1 has been implicated as part of a retrotranslocation channel (54, 56). The size of the channel, however, may not be large enough to accommodate the intact BKV virion (38). For SV40 and MPyV, the current model proposes that oxidoreductases residing in the ER cause conformational changes in the capsid, which in turn lead to ER escape and membrane penetration (35, 48). Once the virus encounters the low-Ca^{2+} environment in the cytosol, further disassembly occurs to aid in genome delivery to the nucleus (48). Whether this model also applies to BKV uncoating requires further investigation.

The involvement of the proteasome during BKV infection is also intriguing. A specific proteasome inhibitor, lactacystin, reduces the infectivity of BKV but does not block BKV capsid rearrangement or VP1 cleavage. Proteasome function has been associated with multiple entry events of different viruses, including endosomal penetration and nuclear translocation (7, 22, 47, 58), and the specific step at which it is required for BKV infection remains to be determined. Since Derlin-1 is closely associated with ERAD components (30, 31, 56, 57), it is possible that BKV may be transported to the proteasome from the ER via Derlin-1 (Fig. 8, step E). Alternatively, the effect of lactacystin on BKV infection may be indirect by impacting Derlin-1 function.

Our results show a unique pattern of BKV capsid protein rearrangement and cleavage. This observation raises several questions. First, the cellular location(s) of VP1 rearrangement and cleavage is not clear. BFA treatment results in an increased level of overall disulfide bond network breakdown and an accumulation of the VP1** molecule, suggesting that the ER is not the site of either event. Lactacystin treatment has a similar effect on capsid rearrangement and VP1 cleavage, and both drugs have an inhibitory effect on TAg expression. These results imply that the presence of either drug may reroute the virus to a pathway that is more favorable for capsid rearrangement (Fig. 8, step D). Second, specific cleavage products of VP1 are seen during infection (Fig. 4), indicating that cleavage

is not a random event. Identification of the cleavage sites on the VP1 molecules may help us elucidate the mechanism of capsid rearrangement. Third, what triggers the disassembly process remains elusive. Low pH certainly plays a significant role, but other signals such as the presence of host factors or certain cellular environments may also contribute. Our results indicate that the breakdown of the disulfide network and VP1 cleavage occur at similar times, and it would be interesting to examine whether these processes are interdependent. Finally, additional genetic and biochemical analyses are warranted to determine whether the capsid rearrangement process and/or VP1 cleavage detected by our assays represent part of an infectious or noninfectious pathway of BKV infection.

In conclusion, our results show that BKV entry in RPTE cells is a highly regulated process, engaging coordinated interactions between viral structures and cellular components. We demonstrate that BKV infection and capsid rearrangement involve low-pH activation, trafficking to the ER, and components of the ERAD pathway. Understanding these steps at the detailed molecular level will expand our insight on general virus entry mechanisms. Moreover, it may help identify important immune regulators, such as the innate immune receptors that are involved in BKV infection, and offer potential intervention targets for BKV-related diseases.

ACKNOWLEDGMENTS

We thank members of the Imperiale lab and Tsai lab for help with this work, Silas Johnson for assistance with Adobe Illustrator, and Christiane Wobus, Kathy Spindler, and Akira Ono for critical reading of the manuscript. We are extremely grateful to Denise Galloway for the VP1 monoclonal antibody P5G6. We also thank the Center for Live Cell Imaging (CLCI) at the University of Michigan for microscopy assistance.

This work was supported by grant AI060584, awarded to M.J.I. from the NIH, and in part by grant CA 46592, awarded to the University of Michigan Cancer Center from the NIH. M.J. was supported by American Heart Association Postdoctoral Fellowship 0825806G. J.R.A. was supported in part by the F.G. Novy Fellowship.

REFERENCES

1. **Abend, J. R., J. A. Low, and M. J. Imperiale.** 2007. Inhibitory effect of gamma interferon on BK virus gene expression and replication. J. Virol. **81:**272–279.
2. **Ahsan, N., and K. V. Shah.** 2006. Polyomaviruses and human diseases. Adv. Exp. Med. Biol. **577:**1–18.
3. **Ashok, A., and W. J. Atwood.** 2003. Contrasting roles of endosomal pH and the cytoskeleton in infection of human glial cells by JC virus and simian virus 40. J. Virol. **77:**1347–1356.
4. **Bernardi, K. M., M. L. Forster, W. I. Lencer, and B. Tsai.** 2008. Derlin-1 facilitates the retro-translocation of cholera toxin. Mol. Biol. Cell **19:**877–884.
5. **Cubitt, C. L.** 2006. Molecular genetics of the BK virus. Adv. Exp. Med. Biol. **577:**85–95.
6. **Damm, E. M., L. Pelkmans, J. Kartenbeck, A. Mezzacasa, T. Kurzchalia, and A. Helenius.** 2005. Clathrin- and caveolin-1-independent endocytosis: entry of simian virus 40 into cells devoid of caveolae. J. Cell Biol. **168:**477–488.
7. **Delboy, M. G., D. G. Roller, and A. V. Nicola.** 2008. Cellular proteasome activity facilitates herpes simplex virus entry at a postpenetration step. J. Virol. **82:**3381–3390.
8. **Doerries, K.** 2006. Human polyomavirus JC and BK persistent infection. Adv. Exp. Med. Biol. **577:**102–116.
9. **Dörries, K.** 2001. Latent and persistent polyomavirus infection, p. 197–235. *In* K. Khalili and G. L. Stoner (ed.), Human polyomaviruses: molecular and clinical perspectives. Wiley-Liss, New York, NY.
10. **Drachenberg, C. B., J. C. Papadimitriou, R. Wali, C. L. Cubitt, and E. Ramos.** 2003. BK polyoma virus allograft nephropathy: ultrastructural features from viral cell entry to lysis. Am. J. Transplant. **3:**1383–1392.
11. **Dugan, A. S., S. Eash, and W. J. Atwood.** 2005. An N-linked glycoprotein with α(2,3)-linked sialic acid is a receptor for BK virus. J. Virol. **79:**14442–14445.
12. **Dugan, A. S., S. Eash, and W. J. Atwood.** 2006. Update on BK virus entry and intracellular trafficking. Transpl. Infect. Dis. **8:**62–67.
13. **Eash, S., and W. J. Atwood.** 2005. Involvement of cytoskeletal components in BK virus infectious entry. J. Virol. **79:**11734–11741.
14. **Eash, S., W. Querbes, and W. J. Atwood.** 2004. Infection of Vero cells by BK virus is dependent on caveolae. J. Virol. **78:**11583–11590.
15. **Ebert, D. H., J. Deussing, C. Peters, and T. S. Dermody.** 2002. Cathepsin L and cathepsin B mediate reovirus disassembly in murine fibroblast cells. J. Biol. Chem. **277:**24609–24617.
16. **Gilbert, J., W. Ou, J. Silver, and T. Benjamin.** 2006. Downregulation of protein disulfide isomerase inhibits infection by the mouse polyomavirus. J. Virol. **80:**10868–10870.
17. **Gilbert, J. M., and T. L. Benjamin.** 2000. Early steps of polyomavirus entry into cells. J. Virol. **74:**8582–8588.
18. **Gilbert, J. M., I. G. Goldberg, and T. L. Benjamin.** 2003. Cell penetration and trafficking of polyomavirus. J. Virol. **77:**2615–2622.
19. **Groll, M., and R. Huber.** 2004. Inhibitors of the eukaryotic 20S proteasome core particle: a structural approach. Biochim. Biophys. Acta **1695:**33–44.
20. **Harlow, E., P. Whyte, B. R. Franza, Jr., and C. Schley.** 1986. Association of adenovirus early-region 1A proteins with cellular polypeptides. Mol. Cell. Biol. **6:**1579–1589.
21. **Imperiale, M. J., and E. O. Major.** 2007. Polyomaviruses, p. 2263–2298. *In* D. M. Knipe and P. M. Howley (ed.), Fields virology, fifth ed., vol. 2. Lippincott Williams & Wilkins, Philadelphia, PA.
22. **Khor, R., L. J. McElroy, and G. R. Whittaker.** 2003. The ubiquitin-vacuolar protein sorting system is selectively required during entry of influenza virus into host cells. Traffic **4:**857–868.
23. **Kim, J. H., L. Johannes, B. Goud, C. Antony, C. A. Lingwood, R. Daneman, and S. Grinstein.** 1998. Noninvasive measurement of the pH of the endoplasmic reticulum at rest and during calcium release. Proc. Natl. Acad. Sci. USA **95:**2997–3002.
24. **Knowles, W. A.** 2006. Discovery and epidemiology of the human polyomaviruses BK virus (BKV) and JC virus (JCV). Adv. Exp. Med. Biol. **577:**19–45.
25. **Li, P. P., A. Naknanishi, M. A. Tran, K. Ishizu, M. Kawano, M. Phillips, H. Handa, R. C. Liddington, and H. Kasamatsu.** 2003. Importance of Vp1 calcium-binding residues in assembly, cell entry, and nuclear entry of simian virus 40. J. Virol. **77:**7527–7538.
26. **Li, T. C., N. Takeda, K. Kato, J. Nilsson, L. Xing, L. Haag, R. H. Cheng, and T. Miyamura.** 2003. Characterization of self-assembled virus-like particles of human polyomavirus BK generated by recombinant baculoviruses. Virology **311:**115–124.
27. **Liddington, R. C., Y. Yan, J. Moulai, R. Sahli, T. L. Benjamin, and S. C. Harrison.** 1991. Structure of simian virus 40 at 3.8-A resolution. Nature **354:**278–284.
28. **Liebl, D., F. Difato, L. Hornikova, P. Mannova, J. Stokrova, and J. Forstova.** 2006. Mouse polyomavirus enters early endosomes, requires their acidic pH for productive infection, and meets transferrin cargo in Rab11-positive endosomes. J. Virol. **80:**4610–4622.
29. **Lilley, B. N., J. M. Gilbert, H. L. Ploegh, and T. L. Benjamin.** 2006. Murine polyomavirus requires the endoplasmic reticulum protein Derlin-2 to initiate infection. J. Virol. **80:**8739–8744.
30. **Lilley, B. N., and H. L. Ploegh.** 2004. A membrane protein required for dislocation of misfolded proteins from the ER. Nature **429:**834–840.
31. **Lilley, B. N., and H. L. Ploegh.** 2005. Multiprotein complexes that link dislocation, ubiquitination, and extraction of misfolded proteins from the endoplasmic reticulum membrane. Proc. Natl. Acad. Sci. USA **102:**14296–14301.
32. **Lippincott-Schwartz, J., and W. Liu.** 2006. Insights into COPI coat assembly and function in living cells. Trends Cell Biol. **16:**e1–e4.
33. **Low, J., H. D. Humes, M. Szczypka, and M. Imperiale.** 2004. BKV and SV40 infection of human kidney tubular epithelial cells in vitro. Virology **323:**182–188.
34. **Low, J. A., B. Magnuson, B. Tsai, and M. J. Imperiale.** 2006. Identification of gangliosides GD1b and GT1b as receptors for BK virus. J. Virol. **80:**1361–1366.
35. **Magnuson, B., E. K. Rainey, T. Benjamin, M. Baryshev, S. Mkrtchian, and B. Tsai.** 2005. ERp29 triggers a conformational change in polyomavirus to stimulate membrane binding. Mol. Cell **20:**289–300.
36. **Marsh, M., and A. Helenius.** 2006. Virus entry: open sesame. Cell **124:**729–740.
37. **Meier, O., and U. F. Greber.** 2004. Adenovirus endocytosis. J. Gene Med. **6**(Suppl. 1)**:**S152–S163.
38. **Meusser, B., C. Hirsch, E. Jarosch, and T. Sommer.** 2005. ERAD: the long road to destruction. Nat. Cell Biol. **7:**766–772.
39. **Moriyama, T., J. P. Marquez, T. Wakatsuki, and A. Sorokin.** 2007. Caveolar endocytosis is critical for BK virus infection of human renal proximal tubular epithelial cells. J. Virol. **81:**8552–8562.
40. **Moriyama, T., and A. Sorokin.** 2008. Intracellular trafficking pathway of BK virus in human renal proximal tubular epithelial cells. Virology **371:**336–349.
41. **Norkin, L. C., H. A. Anderson, S. A. Wolfrom, and A. Oppenheim.** 2002. Caveolar endocytosis of simian virus 40 is followed by brefeldin A-sensitive

transport to the endoplasmic reticulum, where the virus disassembles. J. Virol. **76:**5156–5166.
42. **Pelkmans, L., T. Burli, M. Zerial, and A. Helenius.** 2004. Caveolin-stabilized membrane domains as multifunctional transport and sorting devices in endocytic membrane traffic. Cell **118:**767–780.
43. **Pelkmans, L., J. Kartenbeck, and A. Helenius.** 2001. Caveolar endocytosis of simian virus 40 reveals a new two-step vesicular-transport pathway to the ER. Nat. Cell Biol. **3:**473–483.
44. **Pelkmans, L., D. Puntener, and A. Helenius.** 2002. Local actin polymerization and dynamin recruitment in SV40-induced internalization of caveolae. Science **296:**535–539.
45. **Querbes, W., B. A. O'Hara, G. Williams, and W. J. Atwood.** 2006. Invasion of host cells by JC virus identifies a novel role for caveolae in endosomal sorting of noncaveolar ligands. J. Virol. **80:**9402–9413.
46. **Richterová, Z., D. Liebl, M. Horak, Z. Palkova, J. Stokrova, P. Hozak, J. Korb, and J. Forstova.** 2001. Caveolae are involved in the trafficking of mouse polyomavirus virions and artificial VP1 pseudocapsids toward cell nuclei. J. Virol. **75:**10880–10891.
47. **Ros, C., and C. Kempf.** 2004. The ubiquitin-proteasome machinery is essential for nuclear translocation of incoming minute virus of mice. Virology **324:**350–360.
48. **Schelhaas, M., J. Malmstrom, L. Pelkmans, J. Haugstetter, L. Ellgaard, K. Grunewald, and A. Helenius.** 2007. Simian virus 40 depends on ER protein folding and quality control factors for entry into host cells. Cell **131:**516–529.
49. **Shimura, H., Y. Umeno, and G. Kimura.** 1987. Effects of inhibitors of the cytoplasmic structures and functions on the early phase of infection of cultured cells with simian virus 40. Virology **158:**34–43.
50. **Smith, J. L., S. K. Campos, A. Wandinger-Ness, and M. A. Ozbun.** 2008. Caveolin-1-dependent infectious entry of human papillomavirus type 31 in human keratinocytes proceeds to the endosomal pathway for pH-dependent uncoating. J. Virol. **82:**9505–9512.
51. **Stehle, T., S. J. Gamblin, Y. Yan, and S. C. Harrison.** 1996. The structure of simian virus 40 refined at 3.1 A resolution. Structure **4:**165–182.
52. **Stehle, T., and S. C. Harrison.** 1996. Crystal structures of murine polyomavirus in complex with straight-chain and branched-chain sialyloligosaccharide receptor fragments. Structure **4:**183–194.
53. **Vats, A., P. S. Randhawa, and R. Shapiro.** 2006. Diagnosis and treatment of BK virus-associated transplant nephropathy. Adv. Exp. Med. Biol. **577:**213–227.
54. **Wahlman, J., G. N. DeMartino, W. R. Skach, N. J. Bulleid, J. L. Brodsky, and A. E. Johnson.** 2007. Real-time fluorescence detection of ERAD substrate retrotranslocation in a mammalian in vitro system. Cell **129:**943–955.
55. **Wiethoff, C. M., H. Wodrich, L. Gerace, and G. R. Nemerow.** 2005. Adenovirus protein VI mediates membrane disruption following capsid disassembly. J. Virol. **79:**1992–2000.
56. **Ye, Y., Y. Shibata, M. Kikkert, S. van Voorden, E. Wiertz, and T. A. Rapoport.** 2005. Inaugural article: recruitment of the p97 ATPase and ubiquitin ligases to the site of retrotranslocation at the endoplasmic reticulum membrane. Proc. Natl. Acad. Sci. USA **102:**14132–14138.
57. **Ye, Y., Y. Shibata, C. Yun, D. Ron, and T. A. Rapoport.** 2004. A membrane protein complex mediates retro-translocation from the ER lumen into the cytosol. Nature **429:**841–847.
58. **Yu, G. Y., and M. M. Lai.** 2005. The ubiquitin-proteasome system facilitates the transfer of murine coronavirus from endosome to cytoplasm during virus entry. J. Virol. **79:**644–648.